

Single-Crystals of B-N Based Covalent Organic Polymers with Dual Photosensitive Motifs for Photocatalytic Dye Degradation

Xinpeng He^{†a}, Linkuo Li^{†a}, Qichun Zhang^{*,a,b}

[†] These authors contributed equally to this work.

^a Department of Materials Science and Engineering, City University of Hong Kong, Hong Kong SAR 999077, China.

^b Department of Chemistry, Center of Super-Diamond and Advanced Films (COSDAF) & Hong Kong Institute of Clean Energy (HKICE), City University of Hong Kong, Tat Chee Avenue, Kowloon Tong, Hong Kong SAR, P. R. China

* Email: qiczhang@cityu.edu.hk

1. Materials and methods

All chemicals and solvents were used directly without purification if not specified. PXRD pattern was collected by Rigaku X-ray Diffractometer Smatlab™ 9kW. UV-Vis spectra (300-1500 nm) were measured on Hitachi UH4150 UV-VIS-NIR Spectrophotometer. FTIR spectra (4000 to 400 cm⁻¹) were obtained on a Perkin Elmer Spectrum II. The precise molecular structure was determined by the Rigaku XtaLAB PRO II Industrial single-crystal X-ray diffractometer. X-ray photoelectron spectroscopy (XPS) was measured on an ESCALAB 250Xi system from Thermo Scientific.

Synthesis of DPNTCDI

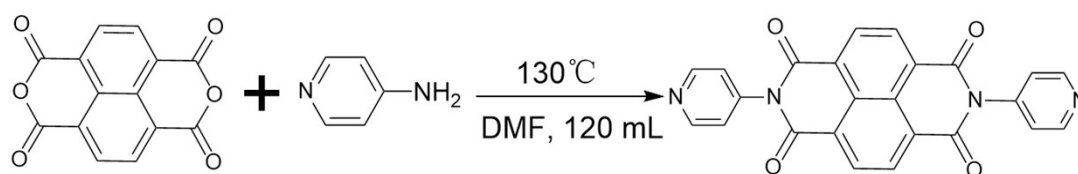


Fig. S1. Synthetic route to DPNTCDI.

1.35 g 1,4,5,8-naphthalenetetracarboxylic dianhydride and 1.18 g 4-aminopyridine were added to 120 mL of DMF in a 250 mL three-necked flask, and the mixture was stirred at 130 °C for at least 12 h under nitrogen protection. After cooling and quenching, the mixture was filtered under reduced pressure, and the precipitate was washed alternately with DMF and acetone until the filtrate became colorless, then dried under vacuum at 100 °C to obtain a solid product.

Synthesis of BDCT

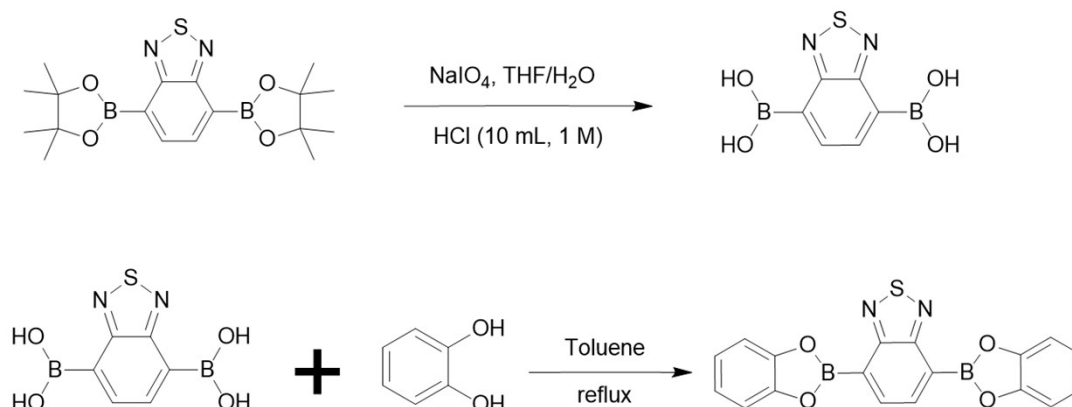


Fig. S2. Synthetic route to BDCT.

Dispersing 2.5 g of 2,1,3-benzothiadiazole-4,7-bis(boronic acid pinacol ester) and 0.8 g of sodium periodate in a THF-water mixed solvent (80 mL/20 mL), the mixture was stirred for 30 min under nitrogen protection, then 10 mL of 1 mol/L hydrochloric acid was added and stirring was continued for 24 h. The mixture was evaporated to dryness, and the residue was washed successively with water, hexane and anhydrous diethyl ether, followed by filtration, to afford pale yellow crystals (yield: 97%), which were directly used for subsequent reactions.

Synthesis of CityU-69

7 mg BDCT and 3.5 mg DPNTCDI were mixed in 4 mL chlorobenzene and heated at 100 °C for 12 h. After cooling, the crystals settled, and chlorobenzene was decanted. The crude product was washed with acetone for impurity removal. Further purification was performed with toluene–methanol if needed. The solid was finally collected and dried.

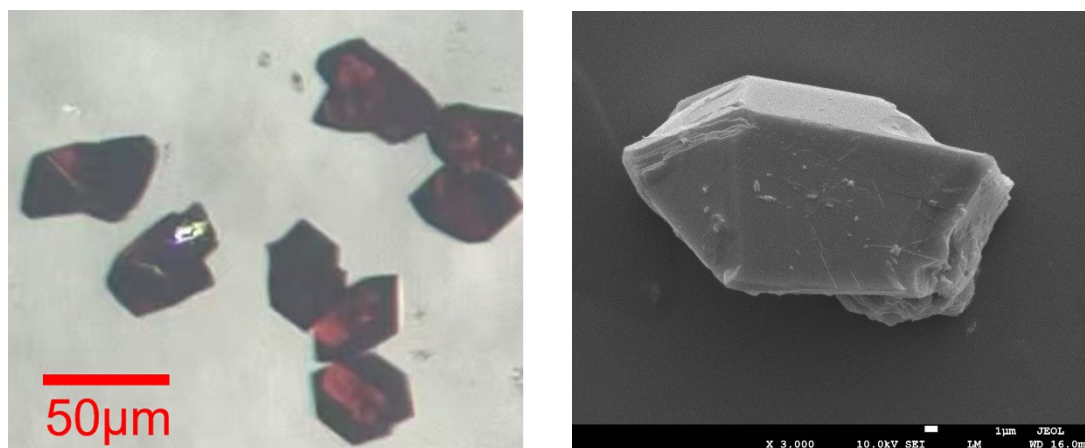


Fig. S3. Optical image and SEM image of CityU-69 crystals.

The two images demonstrate the excellent crystallinity of the material, and the ordered structural arrangement verifies the successful synthesis of CityU-69.

Table. S1. Crystal data and structure refinement of CityU-69.

	CityU-69 (CCDC number: 2534133)
Empirical formula	C ₄₈ H ₂₇ B ₂ N ₆ O ₈ ClS
Formula weight	904.88
Temperature/K	293(2)
Crystal system	orthorhombic
Space group	<i>Pbca</i>
<i>a</i> / Å	15.1673(15)
<i>b</i> / Å	22.553(3)
<i>c</i> / Å	24.122(3)
α / °	90
β / °	90
γ / °	90
Volume / Å ³	8251.2(16)
<i>Z</i>	8
ρ_{calc} g / cm ³	1.457
μ / mm ⁻¹	1.851
<i>F</i> (000)	3712.0
Radiation	CuK α (λ = 1.54184)
2 Θ range for data collection / °	7.33 to 117.868
Index ranges	-16 \leq h \leq 16, -25 \leq k \leq 22, -26 \leq l \leq 26
Reflections collected	28897
Independent reflections	5930 [<i>R</i> _{int} = 0.1503, <i>R</i> _{sigma} = 0.1408]
Data/restraints/parameters	5930/102/596
Goodness-of-fit on <i>F</i> ²	1.000
Final <i>R</i> indexes [<i>I</i> \geq 2 σ (<i>I</i>)]	<i>R</i> ₁ = 0.0864, <i>wR</i> ₂ = 0.2076
Final <i>R</i> indexes [all data]	<i>R</i> ₁ = 0.1912, <i>wR</i> ₂ = 0.2651

$${}^a R_1 = \frac{\sum ||F_o| - |F_c||}{\sum |F_o|}, \quad {}^b wR_2 = \frac{\sum w (|F_o|^2 - |F_c|^2)}{\sum |w(F_o^2)^2|^{1/2}}$$

Table. S2. Selected bond length (Å) for **CityU-69**.

Atom1	Atom2	Length / Å	Atom1	Atom2	Length / Å
S1	N5	1.605(7)	C7	C29	1.377(10)
S1	N6	1.606(7)	C8	C10	1.436(9)
C11	C48	1.789(12)	C8	B1	1.604(10)
O1	C16	1.373(8)	C9	C19	1.391(9)
O1	B1	1.469(9)	C9	C21	1.481(10)
O2	C5	1.366(8)	C10	C22	1.434(10)
O2	B1	1.460(9)	C11	C25	1.484(10)
O3	C17	1.372(8)	C11	C27	1.359(9)
O3	B2	1.486(10)	C12	C28	1.351(9)
O4	C26	1.349(9)	C12	C37	1.360(10)
O4	B2	1.450(10)	N6	C22	1.351(9)
O5	C24	1.218(8)	C14	C22	1.412(10)
N1	C2	1.329(8)	C14	C23	1.373(10)
N1	C6	1.352(8)	C14	B2	1.592(11)
N1	B1	1.666(10)	C15	C24	1.470(10)
O6	C21	1.231(8)	C15	C31	1.376(10)
N2	C18	1.324(9)	C16	C34	1.368(10)
N2	C33	1.333(9)	C17	C26	1.376(11)
N2	B2 ¹	1.685(11)	C17	C40	1.385(11)
N3	C7	1.435(9)	C18	C28	1.374(10)
N3	C24	1.418(9)	C19	C31	1.357(9)
N3	C25	1.405(9)	C20	C30	1.479(10)
O7	C30	1.213(8)	C20	C32	1.362(9)
O8	C25	1.213(8)	C26	C36	1.378(11)

¹3/2-X,1-Y,1/2+Z; ²3/2-X,1-Y,-1/2+Z

Table. S3. Selected bond angles (°) for **CityU-69**.

Atom1	Atom2	Atom3	Angle / °	Atom1	Atom2	Atom3	Angle / °
N5	S1	N6	101.5(4)	C26	C17	C40	121.3(8)
C16	O1	B1	104.3(6)	N2	C18	C28	122.4(7)
C5	O2	B1	104.8(6)	C31	C19	C9	121.2(7)
C17	O3	B2	103.4(6)	C1	C20	C30	120.2(6)
C26	O4	B2	105.7(6)	C32	C20	C1	120.1(7)
C2	N1	C6	117.8(6)	C32	C20	C30	119.8(7)
C2	N1	B1	118.9(6)	O6	C21	N4	118.8(7)
C6	N1	B1	123.0(6)	O6	C21	C9	122.5(7)
C18	N2	C33	118.6(7)	N4	C21	C9	118.7(7)
C18	N2	B2 ¹	121.4(6)	N6	C22	C10	112.2(7)
C33	N2	B2 ¹	120.0(6)	N6	C22	C14	126.8(7)
C24	N3	C7	117.3(6)	C14	C22	C10	121.0(7)
C25	N3	C7	117.6(6)	C14	C23	C4	124.2(7)
C25	N3	C24	124.7(7)	O5	C24	N3	119.3(7)
C21	N4	C12	118.2(6)	O5	C24	C15	124.1(7)
C21	N4	C30	124.4(7)	N3	C24	C15	116.6(7)
C30	N4	C12	117.3(6)	N3	C25	C11	117.0(7)
C3	C1	C20	119.4(6)	O8	C25	N3	120.3(7)
C9	C1	C3	119.2(6)	O8	C25	C11	122.7(7)
C9	C1	C20	121.4(7)	O4	C26	C17	111.0(7)
C10	N5	S1	105.8(5)	O4	C26	C36	127.2(9)
N1	C2	C13	122.9(7)	C17	C26	C36	121.8(8)
C1	C3	C11	118.8(6)	C11	C27	C32	120.4(7)
C1	C3	C15	120.0(6)	C12	C28	C18	118.9(7)

¹3/2-X,1-Y,1/2+Z; ²3/2-X,1-Y,-1/2+Z

The two Level B alerts originate from limited diffraction angle resolution and inherent slight bond precision of the crystal structure, which do not affect the overall structural validity and are acceptable for this material.

XPS Analysis of CityU-69

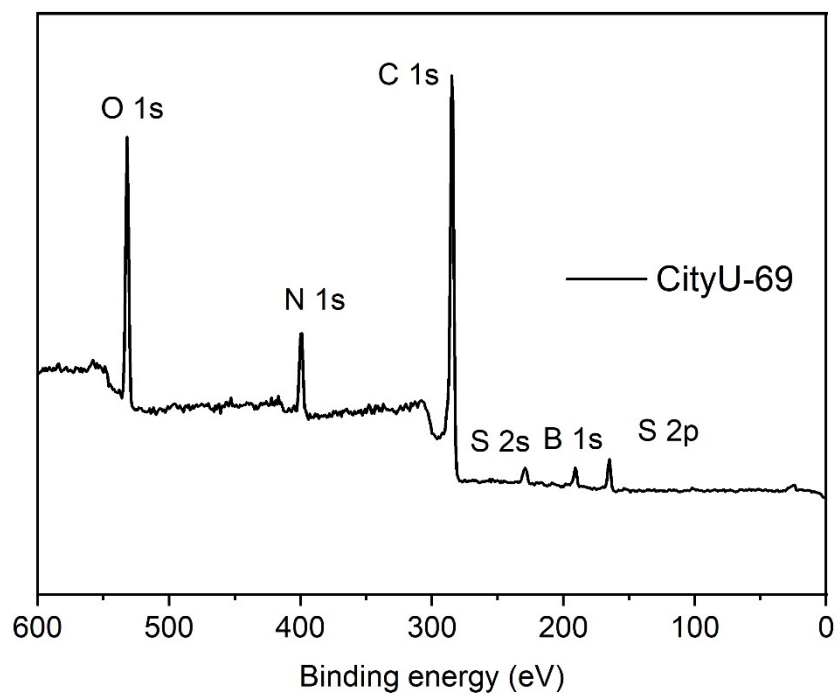


Fig. S4. The XPS survey spectra of CityU-69.

Synthesis and Representation Analysis of CityU-25

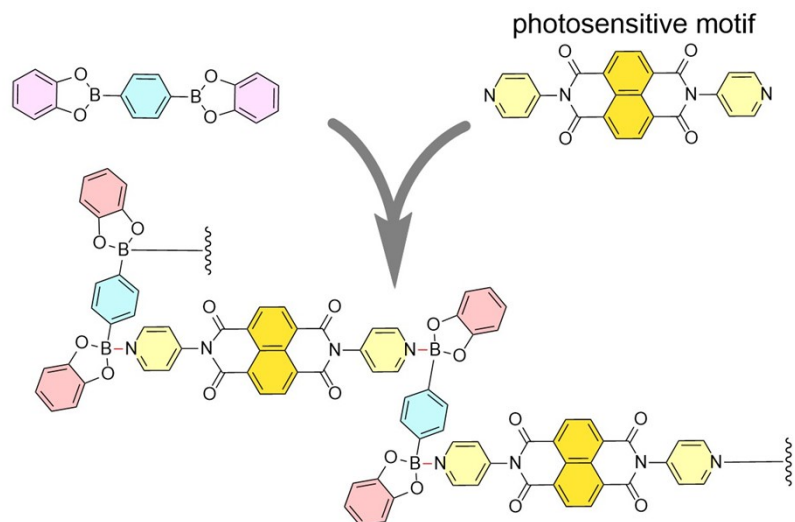


Fig. S5. Synthetic route to CityU-25.

5 mg BACT and 3.5 mg DPNTCDI were dispersed in 4 mL *o*-xylene and heated at 100 °C. After cooling, the solid precipitated, and the supernatant *o*-xylene was decanted. The crude product was rinsed with acetone to remove impurities. Further purification with toluene–methanol was applied if required. The solid was collected and dried.

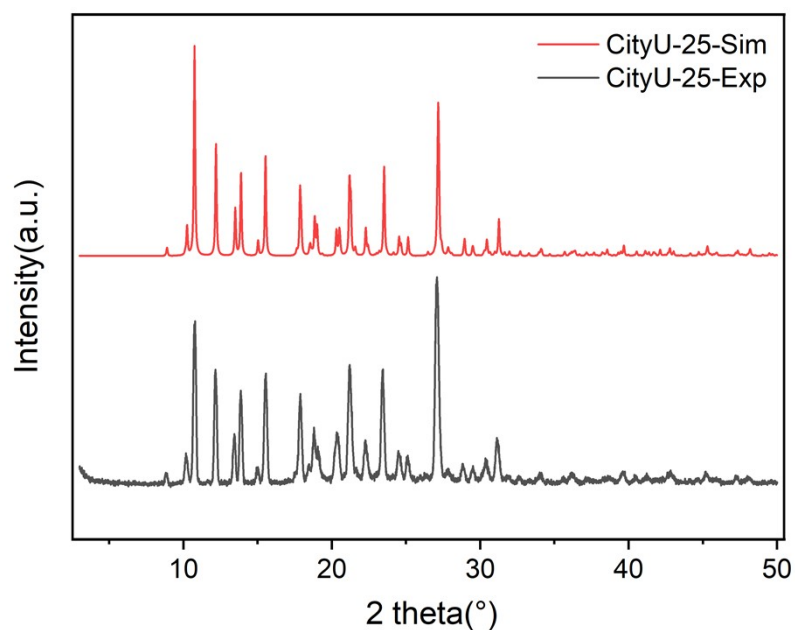


Fig. S6. Simulated and Experimented PXRD patterns of CityU-25.

The experimental pattern was in close agreement with the simulated one, verifying the high purity of CityU-25.

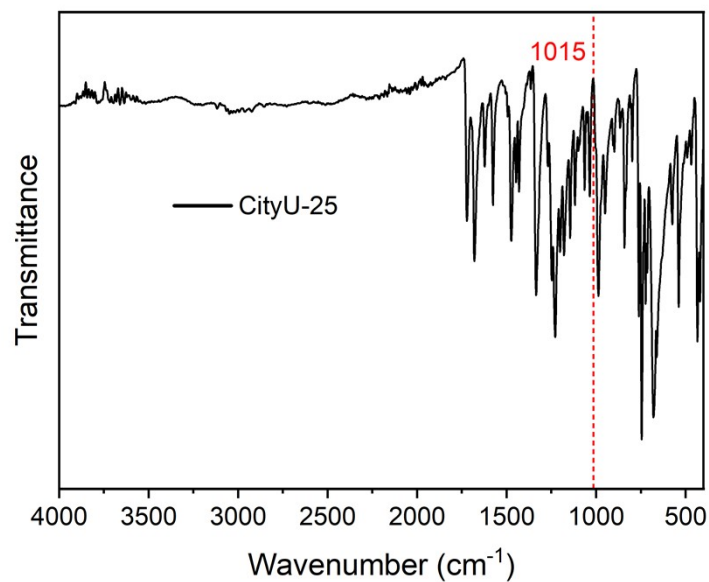


Fig. S7. FTIR spectrum of CityU-25.

Comparison between CityU-69 and CityU-25

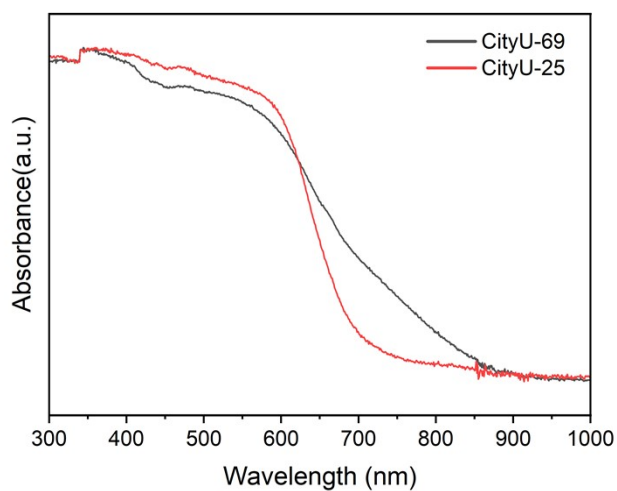


Fig. S8. Comparison of UV-Vis diffuse reflectance spectra between CityU-25 (red) and CityU-69 (black).

2. Experimental Data

Table. S4. MB Degradation Efficiency of Different Photocatalysts after 5 h Irradiation.

Entry	Photocatalysts	Degradation Rate
1	BDCT	73%
2	DPNTCDI	45%
3	BDCT+ DPNTCDI (2:1 by mass)	64%
4	CityU-25	67%
5	CityU-69	77%

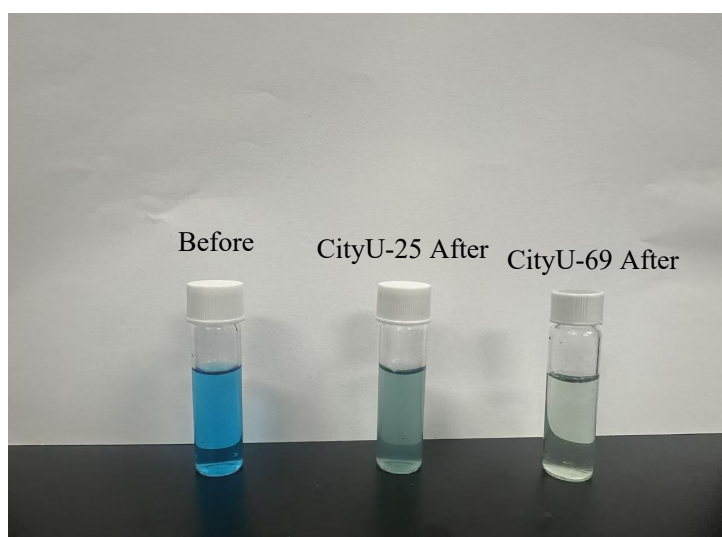


Fig. S9. Qualitative Experimental Data for MB Degradation.

Table. S5. MO Degradation Efficiency of Different Photocatalysts after 5 h Irradiation.

Entry	Photocatalysts	Degradation Rate
1	BDCT	34%
2	DPNTCDI	31%
3	BDCT+ DPNTCDI (2:1 by mass)	23%
4	CityU-25	22%
5	CityU-69	38%

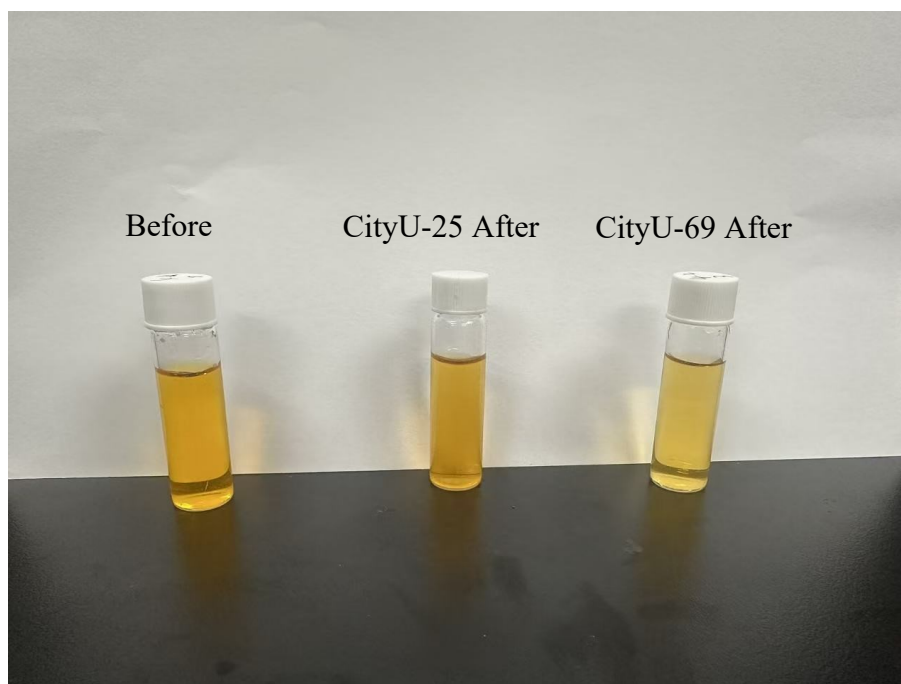


Fig. S10. Qualitative Experimental Data for MO Degradation.

20 ppm aqueous solutions of methylene blue (MB) and methyl orange (MO) were prepared as target substrates. The photocatalytic reactions were performed in glass bottles with a total reaction time of 6 h, and samples were collected 5 times for all systems. CityU-69 was used as the target catalyst, CityU-25 as the reference catalyst, and the raw materials BDCT, DPNTCDI as well as BDCT + DPNTCDI (2:1 by mass) as control samples. The reaction conditions are as follows: all photocatalytic tests are performed under visible LED light (325–500 nm, 5 W) with natural ventilation. The reaction vessel is sealed with plastic film and punched with small holes for air exchange, and no additional aeration is supplied during the experiment.

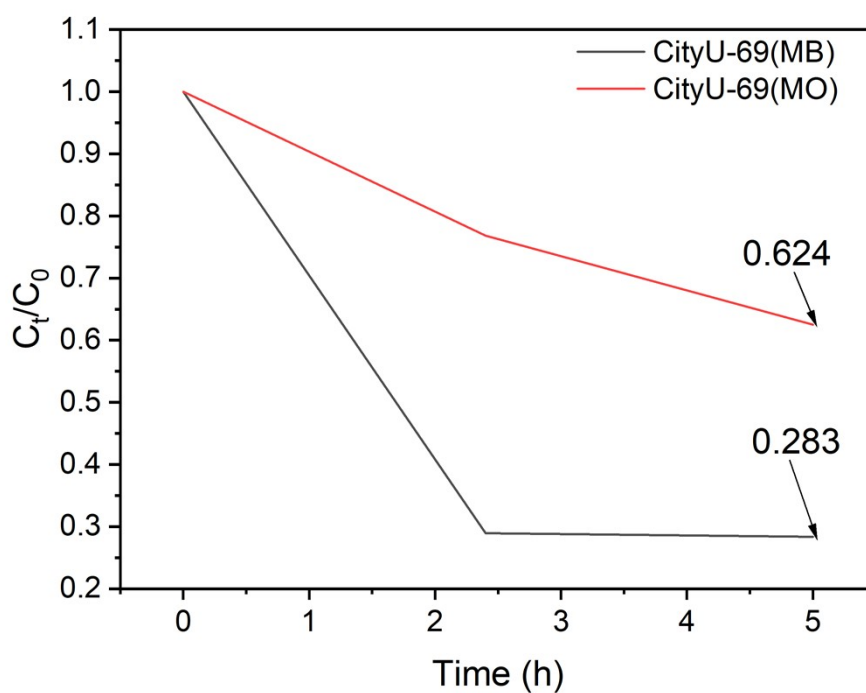


Fig. S11. Relative concentration (C_t/C_0) changes of MB (a) and MO (b) during photocatalytic degradation over CityU-69.

This figure shows the catalytic performance of CityU-69 at a catalyst-to-pollutant mass ratio of 15:1. It can be seen that CityU-69 still exhibits strong catalytic activity even at this relatively low dosage (the ratio used in the main text is 25:1), demonstrating its promising potential for low-cost and high-performance applications.

Table S6. Photocatalytic degradation performance comparison of CityU-69 with reported crystalline COP photocatalysts

Sample	Pollutant	Reaction Condition	Degradation Efficiency	Reference
BC/TiO ₂	MB	100 W, natural	1.89 %/h	[1]
BC/ZnO	MB	100 W, natural	1.71 %/h	[1]
Mg-Zn _{0.07} -g-C ₃ N ₄	MB	60 W, natural	5.2352 %/h	[3]
MnO ₂ /g-C ₃ N ₄	MB	300 W, natural	2.34 %/h	[4]
CityU-69	MB	5 W, pinhole	0.54 %/h	/
BC/TiO ₂	MO	100W, natural	2 %/h	[1]
BC/ZnO	MO	100W, natural	1.83 %/h	[1]
P25	MO	9W, 20 mL/min	7.84 %/h	[2]
ZTO	MO	9W, 20 mL/min	7.04 %/h	[2]
CityU-69	MO	5 W, pinhole	0.37 %/h	/

In the reaction conditions, the first W stands for light source power, and the second parameter is the aeration rate. Natural means an open system with spontaneous air exchange, while pinhole refers to aeration via tiny holes on the plastic sealing film. Reaction efficiency is defined as the pollutant degradation amount within one hour at equal catalyst and pollutant concentrations.

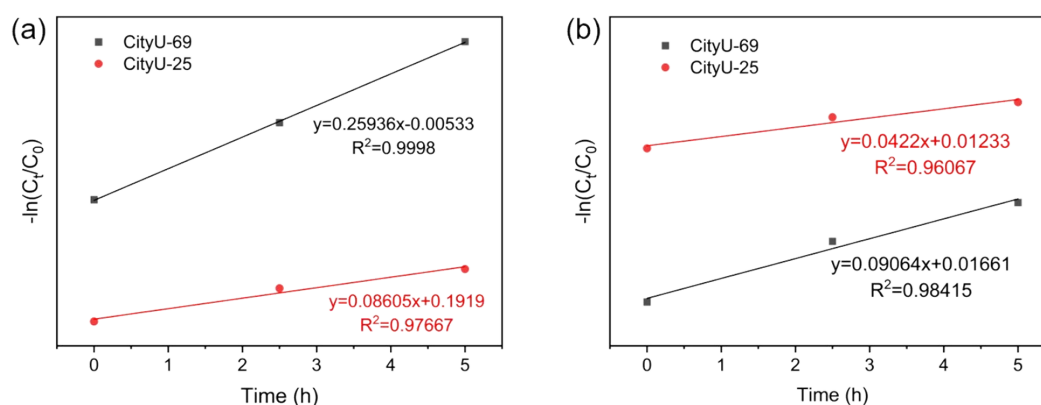


Fig. S12. (a, b) Respective schematic diagram of kinetic fitting for MB and MO degradation

The pseudo-first-order kinetic plots with high R^2 values confirm the reliability of the fitting results. Notably, CityU-69 shows significantly larger rate constants than CityU-25 for both dyes, demonstrating the synergistic effect of its dual photosensitive motifs.

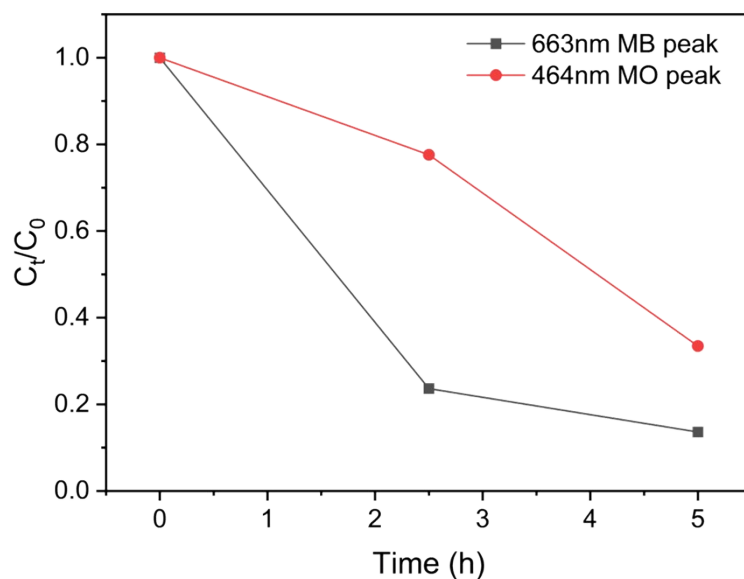


Fig. S13. Variation in (C_t/C_0) of methyl orange and methylene blue upon photocatalytic degradation in binary mixed dye solution

In the mixed system, cationic MB is rapidly adsorbed on the catalyst surface via electrostatic attraction, where it is preferentially degraded by $\bullet\text{OH}$ radicals and h^+ . This frees up surface sites and promotes $\bullet\text{O}_2^-$ generation, accelerating the subsequent degradation of anionic MO.

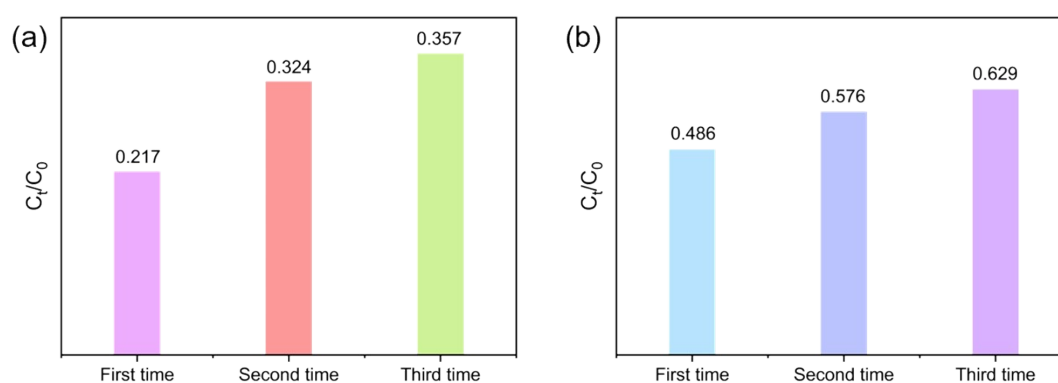


Fig. S14. (a, b) Respective concentration (C_t/C_0) changes of MB and MO during photocatalytic degradation in recycling reaction

The cycling test demonstrates that CityU-69 maintains favorable photocatalytic activity during three consecutive runs. In each cycle, 100 mg of catalyst was added to 200 mL of 20 ppm dye solution and reacted for 6 h. After each reaction, the suspension was centrifuged, and the recovered catalyst was reused with a newly prepared 200 mL

dye solution for the next cycle. Only a slight decline in catalytic performance was observed after three repeated cycles.

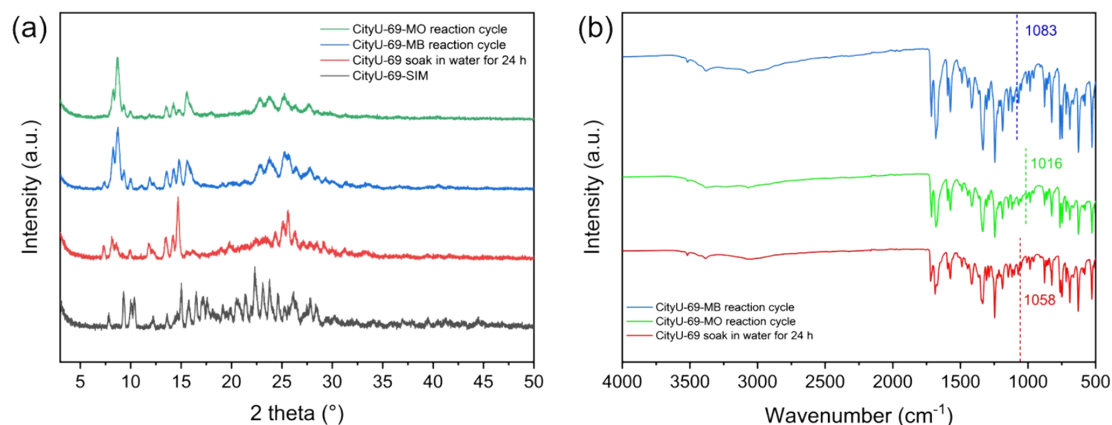


Fig. S15. (a) PXRD of simulated CityU-69 and post-reaction CityU-69; (b) FT-IR spectra of CityU-69 soaking in water for 24 h, MO cycling tests, and MB cycling tests.

To verify the structural stability of the catalyst, the sample was soaked in water (the reaction solvent) for 24 h and then dried. Both the water-soaked sample and the recycled sample after cyclic reactions were characterized by FT-IR and PXRD. The FT-IR spectra confirm that the B←N coordination bonds are well preserved. PXRD patterns indicate that the overall crystallinity of the catalyst remains intact. The slight reduction in peak intensity of the water-soaked sample is probably caused by powder stacking, while the intensity change of the recycled samples results from residual contaminants adsorbed on the surface. Although the catalytic activity decreases slightly after cycling, the catalyst still maintains considerable photocatalytic performance, and it does not react with water to cause deactivation after single use.

Reference

- [1] M. Duan, G. Zeng, J. He and W. Wang, *Diamond Relat. Mater.*, 2023, **137**, 110090.
- [2] S. Shunmugakani, M. S. Prasad, E. Ragulkumar, M. W. Alam, P. Rosaiah, N. G. Prakash and T. J. Ko, *Inorg. Chem. Commun.*, 2024, **168**, 112909.

[3] P. Jiang, L. Zhou, Y. Han, W. Fu, S. Su and M. Zeng, *J. Environ. Chem. Eng.*, 2024, **12**, 112914.

[4] J. Wang, H. Li, S. Meng, L. Zhang, X. Fu and S. Chen, *Appl. Catal., B*, 2017, **200**, 323–330.